

# New Adamantane-like Silicophosphate Cage and Its Reactivity toward Tris(pentafluorophenyl)borane

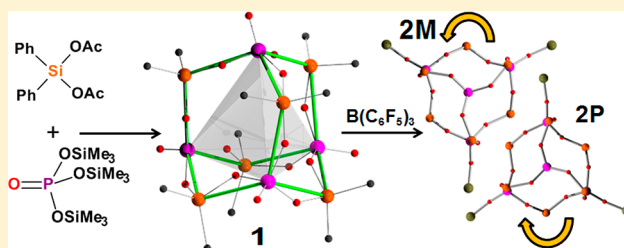
Ales Styskalik,<sup>†,‡</sup> Michal Babiak,<sup>†,‡</sup> Petr Machac,<sup>†</sup> Bohuslava Relichova,<sup>†</sup> and Jiri Pinkas<sup>\*,†,‡,§</sup>

<sup>†</sup>Masaryk University, Department of Chemistry, Kotlarska 2, CZ-61137 Brno, Czech Republic

<sup>‡</sup>Masaryk University, CEITEC MU, Kamenice 5, CZ-62500 Brno, Czech Republic

## Supporting Information

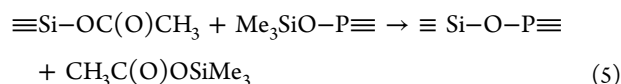
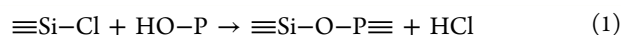
**ABSTRACT:** The condensation reaction between  $\text{Ph}_2\text{Si}(\text{OC}(\text{O})\text{CH}_3)_2$  and  $\text{OP}(\text{OSiMe}_3)_3$  leads to elimination of  $\text{CH}_3\text{C}(\text{O})\text{OSiMe}_3$  and the formation of the new silicophosphate cage molecule  $\text{Ph}_{12}\text{Si}_6\text{P}_4\text{O}_{16}$  (**1**) with an adamantane-like core possessing four terminal  $\text{P}=\text{O}$  moieties and six  $\text{O}-\text{SiPh}_2-\text{O}$  bridging groups. Compound **1** was further reacted with the Lewis acid  $\text{B}(\text{C}_6\text{F}_5)_3$ . We observed adduct formation by coordination through the  $\text{P}=\text{O} \rightarrow \text{B}$  bonds and isolated and structurally characterized two new molecules. In the first of them, the adamantane-like cage is preserved and three phosphoryl oxygen atoms coordinate to boranes, forming  $\text{Ph}_{12}\text{Si}_6\text{O}_{16}\text{P}_4 \cdot 3\text{B}(\text{C}_6\text{F}_5)_3$  (**2**); the remaining  $\text{P}=\text{O}$  group is inverted toward the cage center pointing along a  $\text{C}_3$  molecular axis. The molecule is chiral, and the compound **2** crystallizes as a conglomerate of homochiral crystals. Enantiomers **2M** and **2P** were both structurally characterized. The second adduct resulted from an unexpected reorganization of the  $\text{Si}-\text{O}-\text{P}$  linkages in the adamantane cage during the reaction of **1** with 4 equiv of  $\text{B}(\text{C}_6\text{F}_5)_3$ . The bis-adduct  $\text{Ph}_6\text{Si}_3\text{O}_8\text{P}_2 \cdot 2\text{B}(\text{C}_6\text{F}_5)_3$  (**3**) was formed with an inorganic core representing half of the parent molecule **1**.



## INTRODUCTION

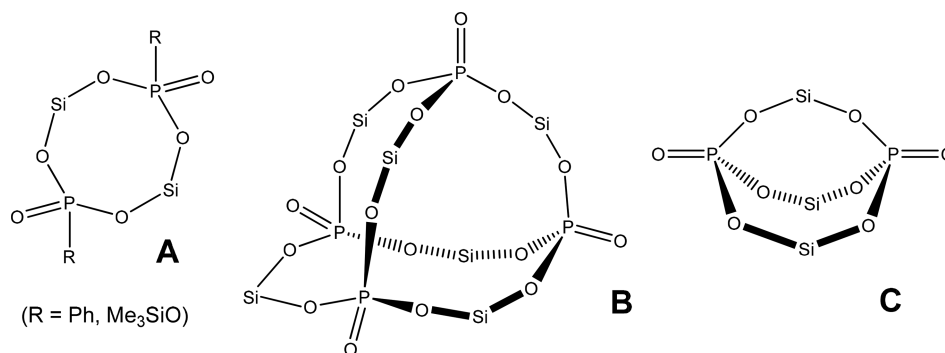
Silicophosphates are compounds containing a network of bridging  $\text{Si}-\text{O}-\text{P}$  bonds between silicate and phosphate moieties. The hydrolytic instability of  $\text{Si}-\text{O}-\text{P}$  bridges limits the available synthetic methods to non-aqueous or high-temperature reactions.<sup>1</sup> The heating of silicon and phosphorus compounds (e.g.,  $\text{SiO}_2$  and  $\text{P}_4\text{O}_{10}$  or  $\text{H}_3\text{PO}_4$ ) leads to reorganization of  $\text{Si}-\text{O}-\text{Si}$  and  $\text{P}-\text{O}-\text{P}$  bonds, condensation between  $\text{Si}-\text{OH}$  and  $\text{P}-\text{OH}$  groups, and water evaporation. The syntheses at increased temperatures provide up to 10 crystalline phases of silicon phosphates.<sup>2–4</sup> Their crystal structures are very similar, which impairs the reproducibility of the synthetic reactions and the purity of their products. The phosphoryl groups in these compounds readily coordinate to silicon atoms, which act as Lewis acids and thus become six-coordinated.<sup>4–6</sup>

The situation becomes significantly different if an organic group is attached to the silicon atom by a stable  $\text{Si}-\text{C}$  bond. Such Si atoms do not acquire octahedral coordination, and bulky organic groups act as steric hindrance to the formation of 3D cross-linked inorganic networks.<sup>7</sup> For these reasons molecular silicophosphates are obtained in the reactions of organosilicon with organophosphorus compounds. Condensation of silicon and phosphorus precursors is performed in nonaqueous solvents under strictly anhydrous conditions in order to prevent the hydrolysis of the newly formed  $\text{Si}-\text{O}-\text{P}$  bonds. Possible reaction pathways include elimination of hydrochloric acid (eqs 1 and 2),<sup>8–10</sup> precipitation of metal halide (eq 3),<sup>11</sup> and alkyl halide elimination (eq 4).<sup>12,13</sup>



We have already reported that the condensation of acetoxysilanes and trimethylsilyl esters of phosphoric and phosphonic acids accompanied by the elimination of trimethylsilyl acetate is suitable for the nonhydrolytic syntheses of a broad variety of silicophosphate xerogels (eq 5).<sup>7,14</sup> Moreover, this reaction principle provided us with the molecular silicophosphate  $[(\text{Ph}_2\text{Si}\{\text{O}_2\text{P}(\text{O})\text{OSiMe}_3\})_2]$  as only the second example of a central  $\text{Si}_2\text{P}_2\text{O}_4$  ring (A in Chart 1),<sup>7</sup> which is similar to the structure obtained by Vaugois et al. by precipitation of metal halide.<sup>11</sup> The hydrolytic instability of silicophosphates still presents a synthetic challenge, and therefore examples of structurally characterized molecular silicophosphates are limited only to trimethylsilyl esters of phosphoric and phosphonic acids and a few other examples, including  $[(\text{Ph}_2\text{Si}\{\text{O}_2\text{P}(\text{O})\text{OSiMe}_3\})_2]$ ,<sup>7</sup>  $[(\text{tBu}_2\text{Si}\{\text{O}_2\text{P}(\text{O})\text{Ph}\})_2]$ ,<sup>11</sup>  $[\text{RSi}(\text{OH})\{\text{OP}(\text{O})(\text{H})(\text{OH})\}]_2\text{O}$

Received: June 30, 2017

Chart 1. Inorganic Cores of Molecular Silicophosphates<sup>a</sup>

<sup>a</sup>Phenyl substituents on Si are omitted for clarity.

(R = (2,6-*i*-Pr<sub>2</sub>C<sub>6</sub>H<sub>3</sub>)NSiMe<sub>3</sub>),<sup>10</sup> and ionic [Et<sub>3</sub>NH]<sub>2</sub>[(Si(PO<sub>4</sub>)<sub>6</sub>(SiO<sub>4</sub>Et<sub>2</sub>)<sub>6</sub>)].<sup>9</sup>

Here we report for the first time the silicophosphate compound **1** with an adamantane-like core (**B** in Chart 1). It was obtained from diacetyldiphenylsilane and tris(trimethylsilyl)phosphate (TTP). The condensation reaction of these two reagents was performed under strictly anhydrous conditions and was accompanied by the elimination of trimethylsilyl acetate, similarly to our previous syntheses of xerogels containing a network of bridging Si–O–P bonds.<sup>7,14</sup> This cage compound **1** with an adamantane-like core was employed in the coordination reactions with the Lewis acid tris(pentafluorophenyl)borane in analogy to already known phosphine oxide–borane adducts.<sup>15,16</sup> Interestingly, the borane not only showed the ability to form P=O→B coordinate bonds but was able to reorganize the P–O–Si bridges as well. This behavior led to two new structures. In **2** the parent adamantane-like cage was maintained, while in **3** a new silicophosphate cage was formed (**C** in Chart 1).

## EXPERIMENTAL SECTION

General experimental methodology and characterization data are described in the Supporting Information.

**Synthesis of Molecular Silicophosphate Ph<sub>12</sub>Si<sub>6</sub>O<sub>16</sub>P<sub>4</sub>·1/4CHCl<sub>3</sub>·9/8C<sub>6</sub>H<sub>6</sub> (1·1/4CHCl<sub>3</sub>·9/8C<sub>6</sub>H<sub>6</sub>).** TTP (3.607 g; 11.47 mmol) was added to a solution of dipenyldiacetyloxysilane (5.065 g; 16.86 mmol) in toluene (20 cm<sup>3</sup>). The reaction mixture was kept at 90 °C for 24 h. Toluene and trimethylsilyl acetate were then removed in vacuo, affording a white viscous liquid. It was gradually heated from room temperature up to 250 °C in vacuo over a period of 8 h. The resulting pale brown solid (mixture of condensation products) was purified by refluxing in benzene. The undissolved white precipitate was filtered off, and after it was dissolved in CDCl<sub>3</sub>, it featured one resonance in the <sup>31</sup>P NMR spectrum (product **1**). It was dried in vacuo and yielded desolvated **1** (3.074 g, 74.2%). A solution of **1** in CHCl<sub>3</sub> was kept in a small open vial placed in a closed flask containing benzene (4 cm<sup>3</sup>; *Caution!* carcinogen). It allowed free diffusion of benzene into chloroform. Crystals of 1·1/4CHCl<sub>3</sub>·9/8C<sub>6</sub>H<sub>6</sub> suitable for an X-ray diffraction analysis were obtained after several days (Figure 1).

**Characterization and Analyses of 1.** <sup>1</sup>H NMR (**1**, CDCl<sub>3</sub>, ppm): δ 7.11–7.52 ((C<sub>6</sub>H<sub>5</sub>)<sub>2</sub>Si, multiplet, 60H). <sup>13</sup>C{<sup>1</sup>H} NMR (**1**, CDCl<sub>3</sub>, ppm): δ 128.1 ((C<sub>6</sub>H<sub>5</sub>)<sub>2</sub>Si, s, para), 128.5 ((C<sub>6</sub>H<sub>5</sub>)<sub>2</sub>Si, s, meta), 131.4 ((C<sub>6</sub>H<sub>5</sub>)<sub>2</sub>Si, s, ortho), 134.5 ((C<sub>6</sub>H<sub>5</sub>)<sub>2</sub>Si, s, ipso). <sup>29</sup>Si NMR (**1**, CDCl<sub>3</sub>, ppm): δ –38.5 ((C<sub>6</sub>H<sub>5</sub>)<sub>2</sub>SiO<sub>2</sub>, s). <sup>31</sup>P NMR (**1**, CDCl<sub>3</sub>, ppm): δ –32.5 (O<sub>3</sub>P=O, s).

IR, MS, TG, elemental analyses, and melting points are given in the Supporting Information.

**NMR-Tube reaction between 1 and B(C<sub>6</sub>F<sub>5</sub>)<sub>3</sub> in a 1:3 Molar Ratio. Molecular Structure of 2·2CHCl<sub>3</sub>.** Compound **1** (50 mg,

0.034 mmol) was dissolved in CDCl<sub>3</sub> (0.45 cm<sup>3</sup>), and then B(C<sub>6</sub>F<sub>5</sub>)<sub>3</sub> (50 mg, 0.098 mmol) was added. It dissolved immediately and formed a slightly yellowish reaction solution. The <sup>31</sup>P NMR spectra were acquired within 15 min of mixing.

<sup>31</sup>P NMR (**1** + 3 B(C<sub>6</sub>F<sub>5</sub>)<sub>3</sub>, ppm): δ –29.6 (s, (SiO)<sub>3</sub>P=O, 1P), –37.2 (broad s, 0.7P), –40.9 (broad s, (SiO)<sub>3</sub>P=O→B(C<sub>6</sub>F<sub>5</sub>)<sub>3</sub> chemical exchange, 18P), –44.9 (broad s, 0.3P), –45.1 (s, 0.1P), –47.1 (s, (SiO)<sub>3</sub>P=O→B(C<sub>6</sub>F<sub>5</sub>)<sub>3</sub>, 0.1P), –54.0 (s, (SiO)<sub>3</sub>P=O→B(C<sub>6</sub>F<sub>5</sub>)<sub>3</sub>, 3P).

The <sup>31</sup>P NMR spectrum after 72 h at room temperature did not change significantly—several new signals of low intensity were observed in the region between –30 and –55 ppm. The relative intensity of the peak at –47.1 ppm increased from 0.1P to 1.5P and continued to grow when we prolonged the reaction time to 2 weeks (Figure 2).

The <sup>31</sup>P NMR spectrum acquired at –60 °C showed splitting of the original broad signal at –40.9 ppm to new, relatively sharp signals at –29.8, –31.1, –48.7, and –50.4 ppm (Figure S2 in the Supporting Information).

We performed the reactions between silicophosphate **1** and tris(pentafluorophenyl)borane also in 1:2, 1:4, and 1:6 ratios and followed their course by <sup>31</sup>P NMR spectroscopy. All spectra showed the three main signals similar to those for the reaction in a 1:3 ratio: –29.6 ppm (s, (SiO)<sub>3</sub>P=O, 1P), –40.9 (broad s, (SiO)<sub>3</sub>P=O→B(C<sub>6</sub>F<sub>5</sub>)<sub>3</sub> chemical exchange, xP), –54.0 (s, (SiO)<sub>3</sub>P=O→B(C<sub>6</sub>F<sub>5</sub>)<sub>3</sub>, 3P), where x decreased with an increasing amount of B(C<sub>6</sub>F<sub>5</sub>)<sub>3</sub> in the reaction mixture. The low-intensity sharp signal at –47.1 ppm grew in all reactions after standing for a few days at room temperature.

Finally, we observed small colorless crystals on the walls of the NMR tube with the reaction mixture of **1** and B(C<sub>6</sub>F<sub>5</sub>)<sub>3</sub> (1:3) after a few days at room temperature. The molecular structure of this product was determined by a single-crystal X-ray diffraction analysis as Ph<sub>12</sub>Si<sub>6</sub>O<sub>16</sub>P<sub>4</sub>·3B(C<sub>6</sub>F<sub>5</sub>)<sub>3</sub>·2CHCl<sub>3</sub> (2·2CHCl<sub>3</sub>, Figure 3).

Crystals of 2·2CHCl<sub>3</sub> were decanted and redissolved in CDCl<sub>3</sub>. Their <sup>31</sup>P NMR spectrum was almost identical with what we observed after mixing of silicophosphate cage **1** with tris(pentafluorophenyl)borane: –29.6 ppm (s, (SiO)<sub>3</sub>P=O, 1P), –40.9 (broad s, (SiO)<sub>3</sub>P=O→B(C<sub>6</sub>F<sub>5</sub>)<sub>3</sub> chemical exchange, 29P), –47.1 (s, (SiO)<sub>3</sub>P=O→B(C<sub>6</sub>F<sub>5</sub>)<sub>3</sub>, 12P), –54.0 (s, (SiO)<sub>3</sub>P=O→B(C<sub>6</sub>F<sub>5</sub>)<sub>3</sub>, 3P).

IR and MS data of 2·2CHCl<sub>3</sub> are given in the Supporting Information.

**Synthesis of Silicophosphate Ph<sub>6</sub>Si<sub>3</sub>O<sub>8</sub>P<sub>2</sub>·2B(C<sub>6</sub>F<sub>5</sub>)<sub>3</sub>·2C<sub>6</sub>H<sub>6</sub> (3·2C<sub>6</sub>H<sub>6</sub>).** Ph<sub>12</sub>Si<sub>6</sub>O<sub>16</sub>P<sub>4</sub> (**1**; 250 mg, 0.170 mmol) was dissolved in CHCl<sub>3</sub> (2 cm<sup>3</sup>), and then B(C<sub>6</sub>F<sub>5</sub>)<sub>3</sub> was added (347 mg, 0.678 mmol). It dissolved immediately and formed a slightly yellowish reaction solution. It was kept in a small open vial placed in a closed flask containing benzene (4 cm<sup>3</sup>; *Caution!* carcinogen). This allowed free diffusion of benzene into chloroform. Colorless crystals of 3·2C<sub>6</sub>H<sub>6</sub> were obtained in the small vial after 1 week with a yield of 150 mg (23.1%); the molecular structure of this product was determined by a single-crystal X-ray diffraction analysis (Figure 4).

**Characterization and analyses of 3·2C<sub>6</sub>H<sub>6</sub>.** <sup>31</sup>P NMR (3·2C<sub>6</sub>H<sub>6</sub>, CDCl<sub>3</sub>, immediately after dissolution, ppm): δ -46.7 (s, (SiO)<sub>3</sub>P=O→B(C<sub>6</sub>F<sub>5</sub>)<sub>3</sub>). The spectrum after standing overnight was almost identical with what we observed in NMR reactions of silicophosphate cage **1** and tris(pentafluorophenyl)borane. It showed the three main signals and only a low-intensity resonance coming probably from the original crystals: -29.6 ppm (s, **2**; (SiO)<sub>3</sub>P=O, 1P), -40.9 (broad s, (SiO)<sub>3</sub>P=O→B(C<sub>6</sub>F<sub>5</sub>)<sub>3</sub> chemical exchange, 40P), -47.1 (s, **3**; (SiO)<sub>3</sub>P=O→B(C<sub>6</sub>F<sub>5</sub>)<sub>3</sub>, 0.6P), -54.0 (s, **2**; (SiO)<sub>3</sub>P=O→B(C<sub>6</sub>F<sub>5</sub>)<sub>3</sub>, 3P).

IR, MS, TG, elemental analyses, and melting points are given in the Supporting Information.

**Crystallography.** Single crystals suitable for diffraction experiments were picked (using LithoLoops) from samples immersed in silicone oil. For all structures (unless explicitly specified), all non-hydrogen atoms were refined anisotropically. Hydrogen atoms were placed in calculated positions, with their *U*<sub>iso</sub> values set to 1.2 times the *U*<sub>eq</sub> value of the carrier atom and refined as riding. Selected crystallographic data are gathered in Table S1 in the Supporting Information.

The molecule **1** (Figure 1) crystallizes as a solvate with CHCl<sub>3</sub> and C<sub>6</sub>H<sub>6</sub>. The symmetrically independent part of the unit cell contains one-third of the molecular fragment of **1** lying on a special position (3-fold screw axis passing through P2\_2) and another whole molecule **1** lying on a general position. Both fragments exhibit positional disorder. The disorder was treated with appropriate geometry restraints and atomic displacement parameter restraints with the sums of individual corresponding parts set to 100%. Solvent that could not be modeled reasonably was treated by the SQUEEZE<sup>17,18</sup> procedure. Finally, an R1 index of slightly over 5% was reached. It is possible that the R1 index could be further lowered by treating other currently ordered atoms as disordered, but the ratios of site occupancy factors already reached values as low as 14.7%/85.3%. The highest peak in the *F*<sub>o</sub> - *F*<sub>c</sub> difference Fourier map is as low as 0.83 e Å<sup>-3</sup>; therefore, the refinement was terminated at this state.

The molecule **2** (Figure 3) crystallizes as a solvate with 2 equiv of CHCl<sub>3</sub>. The main fragment and both solvent molecules lie on special positions (3-fold proper rotation axes passing through the P2–O6 bond and CDCl<sub>3</sub> C–D bonds, respectively). The deuterium scattering factor type is assigned to the trichloromethane hydrogens only. The structure crystallizes in the noncentrosymmetric space group R3; the Flack parameter values -0.027(71) and 0.001(28) confirm the correct absolute structure assignment of both characterized crystals (enantiomers M and P, respectively, Figure 4). The refinement was straightforward.

The molecule **3** (Figure 5) crystallizes as a solvate with 2 equiv of C<sub>6</sub>H<sub>6</sub>. A small part of the low-angle reflections is missing from the data set due to the beam stop setting and detector pixel overflows. The refinement was straightforward.

## RESULTS AND DISCUSSION

**Molecular Silicophosphate Ph<sub>12</sub>Si<sub>6</sub>O<sub>16</sub>P<sub>4</sub> (**1**).** The reaction of TTP and diphenyldiacetoxysilane (eq 6) produced a mixture of molecular oligomeric products at 90 °C. One of them, *trans*-[(Ph<sub>2</sub>Si{O<sub>2</sub>P(O)OSiMe<sub>3</sub>}<sub>2</sub>)]<sub>2</sub>, crystallized out of the reaction mixture and was isolated and characterized; its molecular structure has already been reported.<sup>7</sup> In this molecular product, condensation stops when a centrosymmetric Si<sub>2</sub>P<sub>2</sub>O<sub>4</sub> core (A in Chart 1) is formed. The ring is in a chair conformation, similar to what is observed in the related [(<sup>t</sup>Bu<sub>2</sub>Si{O<sub>2</sub>P(O)Ph})<sub>2</sub>].<sup>11</sup> When the reaction mixture containing molecular products of condensation was further heated without any solvent up to 250 °C, a pale brown solid was obtained. It was recrystallized from hot benzene and dried in vacuo, providing the white product **1** in good yield. Colorless crystals suitable for an X-ray diffraction analysis were obtained by crystallization from a CHCl<sub>3</sub>/C<sub>6</sub>H<sub>6</sub> solution after standing at room temperature for several days. This compound has been

spectroscopically characterized and its molecular structure determined by a single-crystal X-ray diffraction analysis (Figure 1). Selected bond and angle parameters are gathered in Table 1.

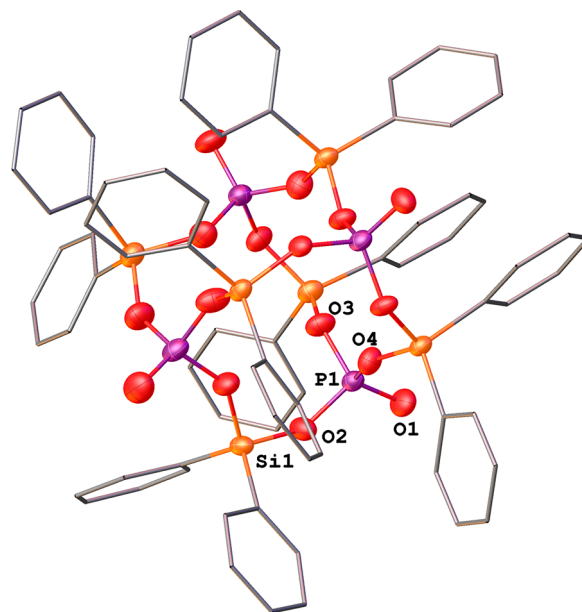
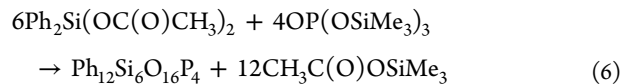


**Figure 1.** Molecular structure of **1**. Solvent molecules, all hydrogen atoms, and another symmetrically independent molecule of **1** are omitted for clarity. Atoms forming the silicophosphate cage are drawn as temperature ellipsoids (50% probability); other (phenyl) moieties are represented using stick models.

In this molecular product, condensation reaction proceeded further beyond [(Ph<sub>2</sub>Si{O<sub>2</sub>P(O)OSiMe<sub>3</sub>}<sub>2</sub>)]<sub>2</sub>; all acetoxy and trimethylsilyl groups reacted and were completely eliminated (eq 6). The novel silicophosphate cage **1**, which has not been reported previously, was formed. It consists of four P=O phosphoryl groups connected through six O–SiPh<sub>2</sub>–O bridges, forming an adamantane-like cage (B in Chart 1). The geometry of two symmetrically independent molecules is approximately tetrahedral, although (in agreement with lower site symmetry) there is some distortion: e.g., P–P intramolecular distances are not equal. Due to the disorder, it is not straightforward to describe this simply by enumeration of P–P distances. However, the molecule retains tetrahedral symmetry in solution, as confirmed by <sup>1</sup>H, <sup>13</sup>C, and <sup>31</sup>P NMR spectra (see below). The inorganic Si<sub>6</sub>O<sub>16</sub>P<sub>4</sub> core (B in Chart 1) is surrounded by phenyl groups bound to Si atoms. Phosphoryl groups are directed outside the cage and are available for the formation of coordination bonds.



The silicon as well as the phosphorus centers are slightly distorted from tetrahedral coordination; the inner ring O2–Si1–O4 (102.51(9)°) and O4–P1–O3 (104.11(11)°) angles deviate only slightly from the ideal values (Table 1). The angles at the oxygen centers O2, O3, and O4 are large (Table 1, 131.27(12)–150.36(13)°), similarly to previously reported cyclic molecular silicophosphates (142.02(8) and 144.60(8)°;<sup>7</sup> 146.1(2) and 148.8(2)°<sup>11</sup>). The Si1–O2 (1.6561(18) Å) and terminal P1=O1 bond lengths (1.455(2) Å), as well as the other P1–O4 distances (1.5541(18) Å), are comparable to

Table 1. Comparison of Selected Bond Distances (Å) and Bond Angles (deg) for Silicophosphates 1, 2P, and 3

$\text{Ph}_{12}\text{Si}_6\text{O}_{16}\text{P}_4 \cdot 1/4\text{CHCl}_3 \cdot 9/8\text{C}_6\text{H}_6$ ( $1 \cdot 1/4\text{CHCl}_3 \cdot 9/8\text{C}_6\text{H}_6$ ) <sup>a</sup>		$\text{Ph}_{12}\text{Si}_6\text{O}_{16}\text{P}_4 \cdot 3\text{B}(\text{C}_6\text{F}_5)_3 \cdot 2\text{CHCl}_3$ ( $2 \cdot 2\text{CHCl}_3$ ) <sup>b</sup>		$\text{Ph}_6\text{Si}_3\text{O}_8\text{P}_2 \cdot 2\text{B}(\text{C}_6\text{F}_5)_3 \cdot 2\text{C}_6\text{H}_6$ ( $3 \cdot 2\text{C}_6\text{H}_6$ )	
P1=O1	1.455(2)	P1=O1	1.480(2)	P1=O1	1.4787(14)
P1-O2	1.5585(18)	P1-O2	1.535(2)	P1-O2	1.5365(14)
P1-O3	1.551(2)	P1-O3	1.538(2)	P1-O3	1.5464(14)
P1-O4	1.5541(18)	P1-O4	1.543(2)	P1-O4	1.5401(14)
		P2=O6	1.463(4)		
		P2-O5	1.564(2)		
Si1-O2	1.6561(18)	Si1-O2	1.663(2)	Si1-O2	1.6715(14)
Si1-O4	1.6639(18)	Si1-O4	1.675(2)	Si1-O6	1.6743(14)
Si2-O3	1.633(2)	Si2-O3	1.676(2)		
		Si2-O5	1.655(2)		
		B1-O1	1.542(4)	B1-O1	1.566(3)
O1-P1-O4	113.92(12)	O1-P1-O2	109.68(12)	O1-P1-O2	110.69(8)
O1-P1-O3	115.57(13)	O1-P1-O3	111.35(13)	O1-P1-O3	110.92(8)
O4-P1-O3	104.11(11)	O2-P1-O4	106.89(12)	O2-P1-O4	109.03(8)
		O5-P2-O5	104.29(10)		
		O6-P2-O5	114.26(9)		
O2-Si1-O4	102.51(9)	O2-Si1-O4	105.66(11)	O2-Si1-O6	103.29(7)
		O3-Si2-O5	106.45(11)		
		B1-O1-P1	159.0(2)	B1-O1-P1	142.01(13)
P1-O2-Si1	131.27(12)	P1-O2-Si1	152.33(15)	P1-O2-Si1	147.95(10)
P1-O3-Si2	150.36(13)	P2-O5-Si2	132.90(15)	P1-O3-Si2	139.38(9)

<sup>a</sup>Bond lengths and angles for  $1 \cdot 1/4\text{CHCl}_3 \cdot 9/8\text{C}_6\text{H}_6$  are listed for residue 2 (atom names with suffix “\_2”). In cases where the structure contains more chemically equivalent bond lengths, one representative value was chosen. A full listing of bond lengths can be found in the CIF files. <sup>b</sup>Data given in the table are for enantiomer **2P** (CCDC 1555739); bond lengths and angles for **2M** are virtually the same and can be found in the CIF file (CCDC 1558817).

those found in other molecular silicophosphates and crystalline silicon phosphates.<sup>4,11</sup>

Both <sup>31</sup>P and <sup>29</sup>Si NMR spectra reveal only one resonance with the expected chemical shifts, and all four peaks of monosubstituted phenyl rings (ortho, meta, para, ipso) are observed in the <sup>13</sup>C{<sup>1</sup>H} NMR spectrum. The <sup>1</sup>H NMR spectrum displays a multiplet in the aromatic region (7.11–7.52 ppm). All NMR spectra agree well with the discussed structure. IR spectroscopic data<sup>19</sup> and elemental analyses are consistent with the results of X-ray diffraction analysis. In addition, the APCI-MS spectrum of **1** shows the molecular peak of the silicophosphate cage at 1474 *m/z*, while EI-MS contains only signals of cage fragments (see the Supporting Information).

**NMR-Tube Reaction between 1 and B(C<sub>6</sub>F<sub>5</sub>)<sub>3</sub> in a 1:3 Molar Ratio. Molecular Structure of 2·2CHCl<sub>3</sub>.** As already mentioned, the phosphoryl oxygen atoms of silicophosphate cage **1** are directed outward and therefore we tried to use them in coordination reactions with the very strong Lewis acid tris(pentafluorophenyl)borane. We observed an immediate reaction between the cage and borane after mixing in the <sup>31</sup>P NMR spectra (Figure 2). The predicted coordination of phosphoryl oxygen to boron was anticipated to occur quickly, and this is in agreement with an instantaneous change in the NMR spectra. It was noteworthy that the <sup>31</sup>P NMR spectra were very similar for all the reactions performed at different 1:B(C<sub>6</sub>F<sub>5</sub>)<sub>3</sub> ratios (1:2, 1:3, 1:4, and 1:6). We always observed two sharp resonances at –29.6 and –54.0 ppm, which held a constant 1:3 intensity ratio, and a broad intense signal at –40.9 ppm. After standing for a few days at room temperature, a fourth significant signal appeared in all reaction solutions at –47.1 ppm (Figure 2). On the basis of the NMR shifts, the phosphoryl groups featuring a peak at –29.6 ppm belong

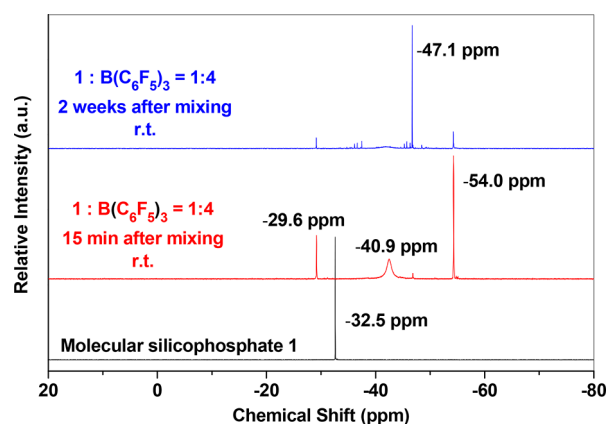
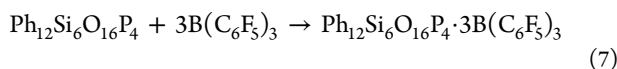


Figure 2. <sup>31</sup>P NMR spectra of the reaction of molecular silicophosphate **1** and tris(pentafluorophenyl)borane in a molar ratio of 1:4.

probably to uncoordinated P=O moieties, similar to the starting cage **1**, which shows a chemical shift of –32.5 ppm. The other signals are shifted upfield from the original resonance by 8–22 ppm, attesting to the coordination of these phosphoryl oxygens to boron.<sup>16</sup> Moreover, the broadness of the signal at –40.9 ppm points to some dynamic exchange processes present in the reaction mixture, which will be discussed later.

Since the 1:3 intensity ratio of the –29.6 and –54.0 ppm resonances was constant and independent of the reaction stoichiometric ratios, reaction times etc., we assumed that a tris-adduct of silicophosphate cage and B(C<sub>6</sub>F<sub>5</sub>)<sub>3</sub> was formed (eq 7). Subsequently, we were able to obtain several crystals from the walls of the NMR tube, which allowed us to determine

molecular structure of **2** by the single crystal X-ray diffraction analysis.



The molecule of compound **2** indeed was an adduct of the parent adamantane-like silicophosphate cage **1** and borane in a 1:3 ratio (Figure 3), as predicted on the basis of the  $^{31}\text{P}$  NMR

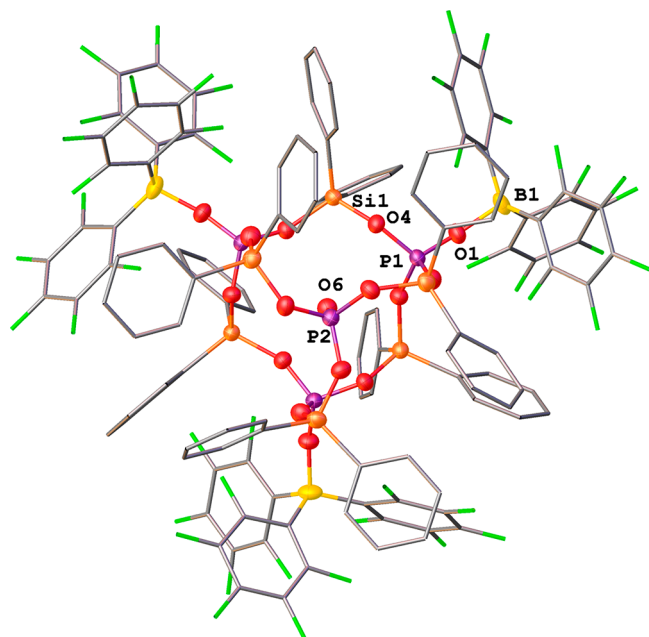


**Figure 3.** Molecular structure of **2P**.  $\text{CDCl}_3$  and hydrogens are omitted for clarity. Atoms forming the silicophosphate cage including boron atoms are drawn as temperature ellipsoids (50% probability); other (phenyl and pentafluorophenyl) moieties are represented using stick models.

spectra. Interestingly, the fourth phosphoryl group remained uncoordinated and, unlike the case for the starting precursor **1**, it is inverted and points inside the silicophosphate cage. This molecule crystallizes as a solvate with two molecules of  $\text{CHCl}_3$  in enantiomorphic space group  $R\bar{3}$  and resembles a propeller with  $C_3$  symmetry. The  $\text{P2}=\text{O6}$  bond coincides with the 3-fold axis, and the molecule is chiral. The crystals, which were characterized by a single-crystal X-ray diffraction analysis, were stereochemically pure on the basis of Flack parameter values ( $-0.027(71)$  and  $0.001(28)$ , respectively). A comparison of the molecular structures of the two characterized crystals (Figure 4) clearly shows that these were built up from opposite enantiomers, which are denoted **2M** and **2P**, respectively, according to IUPAC recommendations regarding axial chirality.<sup>20</sup> The bond lengths, angles, and other crystal structure parameters are virtually equal for both enantiomers. From this point on, we will discuss only the **2P** enantiomer.

The bond lengths and angles of **2P** changed only slightly in comparison to the parent silicophosphate cage **1** after the formation of new coordination bonds (Table 1). The differences in distances between double and single bonds in distorted  $\text{PO}_4$  tetrahedrons (around three equivalent P1 atoms) leveled out—the double  $\text{P}=\text{O}$  bonds are elongated from  $1.455(2)$  to  $1.480(2)$  Å, while the single  $\text{P}-\text{O}$  bonds are shortened ( $1.535(2)$ – $1.543(2)$  Å). The  $\text{O}-\text{P}-\text{O}$  angles moved closer to the ideal tetrahedral values ( $106.89(12)$ –

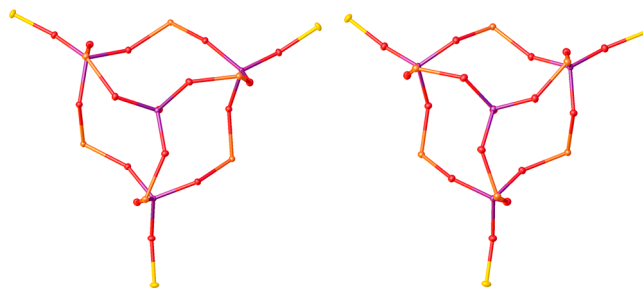


**Figure 4.** Molecular cores of **2P** (left) and **2M** (right) representing opposite enantiomers. Each crystal of **2** is built up solely from one of these enantiomers. The 3-fold axes are perpendicular to the paper.

$111.35(13)^\circ$ ). These changes were not observed at the unique uncoordinated  $\text{PO}_4$  group (around the P2 atom)—this tetrahedron remained more distorted. The  $\text{Si}-\text{O}$  bond lengths and the  $\text{O}-\text{Si}-\text{O}$  and  $\text{P}-\text{O}-\text{Si}$  angles remained virtually unchanged. The  $\text{O}-\text{B}-\text{C}$  and  $\text{C}-\text{B}-\text{C}$  angles were close to the ideal tetrahedral values ranging from  $107.0(3)$  to  $108.2(2)^\circ$  and from  $105.7(3)$  to  $114.5(3)^\circ$ , respectively.

These results can be compared with adducts of  $\text{B}(\text{C}_6\text{F}_5)_3$  with triphenyl- and triethylphosphine oxides, which were fully described by a single-crystal X-ray diffraction analysis.<sup>15,16</sup> In our case, the  $\text{P}=\text{O}$  bond lengths are shorter than those in the reported compounds ( $1.480(2)$  Å vs  $1.497(2)$  and  $1.4973(17)$  Å for  $\text{Ph}_3\text{PO}$  and  $\text{Et}_3\text{PO}$  adducts, respectively) and  $\text{B}-\text{O}$  bond lengths ( $1.542(4)$  Å) are comparable to those in  $\text{Ph}_3\text{PO}$  and  $\text{Et}_3\text{PO}$  adducts ( $1.538(3)$  Å and  $1.533(3)$  Å, respectively). The  $\text{P}-\text{O}-\text{B}$  angle was almost linear ( $178.7(2)^\circ$ ) in the case of  $\text{Ph}_3\text{PO}\cdot\text{B}(\text{C}_6\text{F}_5)_3$ , and this was explained by strong  $\pi-\pi$  stacking interactions between the phenyl rings, which were present in this compound. This was not the case for  $\text{Et}_3\text{PO}\cdot\text{B}(\text{C}_6\text{F}_5)_3$ , with the corresponding angle of  $161.04(16)^\circ$ .<sup>15,16</sup> This value was slightly lower in our case ( $159.0(2)^\circ$ ) and thus very similar to what was observed in the  $\text{Et}_3\text{PO}\cdot\text{B}(\text{C}_6\text{F}_5)_3$  adduct.

NMR spectroscopy and EI-MS analyses (see the Supporting Information) showed that the molecule **2** is quite unstable similarly to **3** (see below). The IR spectra (see the Supporting Information) display clearly the presence of a silicophosphate cage as well as tris(pentafluorophenyl)borane.<sup>19,21–23</sup>

**Molecular Silicophosphate 3.** The most intense resonance in all acquired  $^{31}\text{P}$  NMR spectra was the broad peak at  $-40.9$  ppm. It decreased in intensity after standing for several days at room temperature, while the originally minor signal at  $-47.1$  ppm increased significantly (Figure 2). On the basis of these facts we concluded that some slow reaction leads to a new molecular product with only one resonance in the  $^{31}\text{P}$  NMR spectrum. The existence of a coordinate  $\text{P}=\text{O}\rightarrow\text{B}$  bond was assumed due to the shift to high field in comparison with the precursor. In order to obtain a suitable crystal for the X-ray diffraction analysis, we performed vapor diffusion of benzene (antisolvent) into the mother liquor. The reaction mixture of **1** with  $\text{B}(\text{C}_6\text{F}_5)_3$  in a 1:4 stoichiometric ratio (featuring resonances of **2** and some reaction intermediates in  $^{31}\text{P}$  NMR spectra—mainly the broad signal at  $-40.9$  ppm) deposited colorless crystalline product after standing in a closed vial for several days in a glovebox. It displayed one resonance at  $-47.1$  ppm in the  $^{31}\text{P}$  NMR spectrum measured immediately after dissolution; however, the four signals at  $-29.6$ ,  $-40.9$ ,  $-47.1$ , and  $-54.0$  ppm characteristic for NMR reactions between parent silicophosphate cage **1** and tris(pentafluorophenyl)-

borane were observed after standing in the NMR tube for several hours. Thus, the product was not stable in solution and a single-crystal X-ray diffraction analysis was the most effective and powerful characterization method.

The molecular structure consists of a  $\text{Ph}_6\text{Si}_3\text{O}_8\text{P}_2$  silicophosphate cage and two  $\text{B}(\text{C}_6\text{F}_5)_3$  moieties bound through the coordination  $\text{P}=\text{O} \rightarrow \text{B}$  bonds (Figure 5). However, the cage in

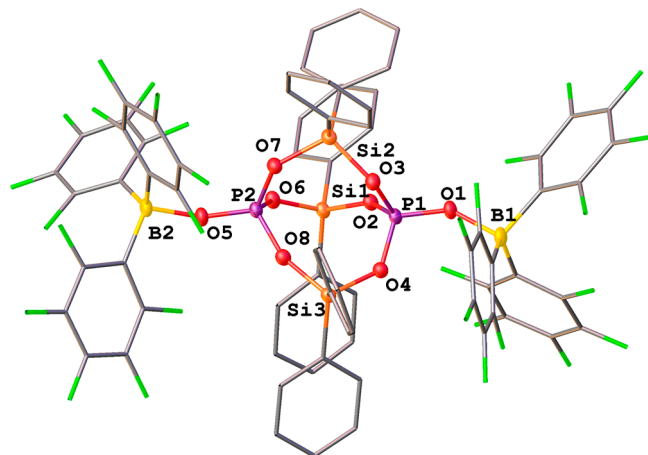
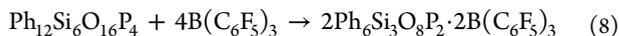


**Figure 5.** Molecular structure of **3**.  $\text{C}_6\text{H}_6$  and hydrogens are omitted for clarity. Atoms forming the silicophosphate cage including boron atoms are drawn as temperature ellipsoids (50% probability); other (phenyl and pentafluorophenyl) moieties are represented using stick models.

this case is only half of the cage **1** we used as a precursor and it contains only two phosphorus atoms connected through three  $\text{O}-\text{SiPh}_2-\text{O}$  bridges. The Si atoms still bear phenyl groups in  $\text{Ph}_2\text{Si}$  moieties. The molecule crystallizes as a solvate with two molecules of benzene (eq 8).



Four  $\text{P}-\text{O}-\text{Si}$  bonds had to be broken and formed again in order to divide the former silicophosphate cage **1** into two new cages **3**. This was effectively but slowly accomplished by the strong Lewis acid  $\text{B}(\text{C}_6\text{F}_5)_3$ . Very strong electron-withdrawing properties of  $\text{B}(\text{C}_6\text{F}_5)_3$ <sup>24</sup> probably weaken the  $\text{P}-\text{O}-\text{Si}$  bridges and allow for their reorganization, which affords the product with relatively low stability in solution.

The reorganization of the  $\text{P}-\text{O}-\text{Si}$  bonds and probably also the instability of the  $\text{P}=\text{O} \rightarrow \text{B}$  coordination bonds lead to the broad signal at  $-40.9$  ppm in the  $^{31}\text{P}$  NMR spectrum, which was only slowly transformed into the sharp peak of the new borane adduct of silicophosphate cage **3**. We assume that the instability of the  $\text{P}=\text{O} \rightarrow \text{B}$  coordination bonds could be one of the possible reasons for the signal broadening in the  $^{31}\text{P}$  NMR spectra, because the broad signal splits at  $-60$  °C into four resonances at  $-29.8$ ,  $-31.1$ ,  $-48.7$ , and  $-50.4$  ppm (Figure S2 in the Supporting Information), which belong to some reaction intermediates. The two downfield signals correspond most likely, according to their chemical shift, to uncoordinated phosphoryl groups.

The bond lengths and angles in **3** differ again only slightly from the previously described structures (Table 1). The double  $\text{P1}=\text{O1}$  bond is only slightly elongated to  $1.4787(14)$  Å, and it is almost similar to the respective bond in silicophosphate-borane adduct **2** ( $1.480(2)$  Å). However, the second double  $\text{P2}=\text{O5}$  bond is significantly shortened to  $1.4668(14)$  Å. The

single  $\text{P}-\text{O}$  bonds are in the range from  $1.5365(14)$  to  $1.5464(14)$  Å. The  $\text{O}-\text{P}-\text{O}$  angles were again close to the ideal tetrahedral values ( $106.76(8)$ – $112.34(8)^\circ$ ). The  $\text{Si}-\text{O}$  bond lengths and the  $\text{O}-\text{Si}-\text{O}$  and  $\text{P}-\text{O}-\text{Si}$  angles remained virtually unchanged. The  $\text{B}-\text{O}$  bonds were longer ( $1.566(3)$  and  $1.570(3)$  Å) in this case in comparison to those in adduct **2**,  $\text{Ph}_3\text{PO} \cdot \text{B}(\text{C}_6\text{F}_5)_3$ , and  $\text{Et}_3\text{PO} \cdot \text{B}(\text{C}_6\text{F}_5)_3$ .<sup>15,16</sup> The  $\text{P}-\text{O}-\text{B}$  angle decreased significantly to  $142.01(13)^\circ$  (in comparison with  $158.94(13)^\circ$  in the case of **2**). The angles around B1 and B2 atoms ( $\text{O}-\text{B}-\text{C}$  and  $\text{C}-\text{B}-\text{C}$ ) were in the range from  $102.48(16)$  to  $115.42(17)^\circ$  and from  $104.42(16)$  to  $115.62(17)^\circ$ , respectively, and deviate more from the ideal tetrahedral values in comparison to molecule **2**. Together with  $\text{P2}=\text{O5}$  bond shortening and elongation of both  $\text{B}-\text{O}$  bonds, this is reasonable evidence for weakening of  $\text{O} \rightarrow \text{B}$  coordination bonds in this case. This fact is in broader agreement with the low stability of this compound in solution, as revealed by NMR and MS analyses (discussed below).

The spectroscopic data agree well with the described adduct structure. In the  $^{31}\text{P}$  NMR spectrum we observed a shift from  $-32.5$  ppm for the parent cage **1** to  $-47.1$  ppm for the new molecule **3** upon coordination to the borane. This is consistent with what is observed in the case of methyl, ethyl, and phenyl esters of phosphoric acid.<sup>16</sup> It is noteworthy that in the case of phosphine oxides the  $^{31}\text{P}$  NMR shifts move in the opposite direction and the extent of the shift is often used as a measure of Lewis acidity.<sup>16</sup> Molecule **3** provides only one signal in its  $^{31}\text{P}$  NMR spectrum because the molecular symmetry in solution increases to the ideal  $D_{3h}$  point group and equilibrates the two phosphorus atom environments observed in the crystal structure. Because of the instability of the compound in solution (see the Experimental Section and discussion above) we were not able to acquire  $^{13}\text{C}$  and  $^{29}\text{Si}$  NMR spectra with sufficient quality. The IR spectra (see the Supporting Information) were described with the help of cited literature<sup>19,21–23</sup> and display clearly the presence of both parts of the molecule—the silicophosphate cage as well as tris(pentafluorophenyl)borane. The shift of absorption band of the  $\text{P}=\text{O}$  stretch to lower wavenumbers upon coordination is probably  $45$   $\text{cm}^{-1}$ , and it is comparable to phosphine oxide adducts with  $\text{B}(\text{C}_6\text{F}_5)_3$ .<sup>16</sup> However, we were not able to distinguish the absorption band of the  $\text{P}=\text{O}$  valence vibration in the parent cage unambiguously because it was overlapped with the absorption band of the  $\text{C}-\text{H}$  bending vibration. Both APCI-MS and EI-MS spectra confirm the low stability of this adduct **3**, as they both show a signal at  $737$   $m/z$  which belongs to the silicophosphate cage  $\text{Ph}_6\text{Si}_3\text{P}_2\text{O}_8$ , without coordinated  $\text{B}(\text{C}_6\text{F}_5)_3$  molecules. Moreover, the EI-MS contains signals of  $\text{B}(\text{C}_6\text{F}_5)_3$  and its fragments. The molecular peak of the adduct **3** was not observed by either method.

## CONCLUSIONS

This work describes the synthesis and complete characterization of new silicophosphate cage molecules. An adamantane-like structure (**1**) with four phosphorus atoms connected via six  $\text{O}-\text{SiPh}_2-\text{O}$  bridges was prepared by nonhydrolytic condensation of  $\text{Ph}_2\text{Si}(\text{OC}(\text{O})\text{CH}_3)_2$  and  $\text{OP}(\text{OSiMe}_3)_3$ . This reaction principle based on  $\text{CH}_3\text{C}(\text{O})\text{OSiMe}_3$  elimination could become useful for the preparation of other molecular silicophosphates and -phosphonates. The four phosphoryl oxygen atoms in **1** are directed outside the cage and offered the possibility for use in coordination chemistry. We reacted this silicophosphate cage **1** with Lewis acidic  $\text{B}(\text{C}_6\text{F}_5)_3$  and

observed both coordination and reorganization of the P–O–Si bonds. Two new products were obtained and structurally characterized by the X-ray diffraction analysis. In the first of them the adamantane-like structure is preserved, and it forms the adduct of **2** with borane in a 1:3 ratio. One phosphoryl oxygen remained free and points inside the cage. The molecule can be described as a chiral  $C_3$  propeller. The compound crystallizes as a conglomerate of homochiral crystals. Crystals of both enantiomers **2P** and **2M** were obtained and structurally characterized. In the second product we observed only half of the parent adamantane-like cage forming the adduct **3** with  $B(C_6F_5)_3$  in a 1:2 ratio. The four P–O–Si bonds had to be broken and formed again during the reaction in order to build this smaller silicophosphate cage. The presented molecules could serve as models for structural building units present in the silicophosphate xerogels. We will be investigating further reactivity modes of **1** with other reagents.

## ■ ASSOCIATED CONTENT

### ● Supporting Information

The Supporting Information is available free of charge on the ACS Publications website at DOI: 10.1021/acs.inorgchem.7b01572.

Characterization details and spectroscopic data (PDF)

### Accession Codes

CCDC 1555739, 1555762–1555763, and 1558817 contain the supplementary crystallographic data for this paper. These data can be obtained free of charge via [www.ccdc.cam.ac.uk/data\\_request/cif](http://www.ccdc.cam.ac.uk/data_request/cif), or by emailing [data\\_request@ccdc.cam.ac.uk](mailto:data_request@ccdc.cam.ac.uk), or by contacting The Cambridge Crystallographic Data Centre, 12 Union Road, Cambridge CB2 1EZ, UK; fax: +44 1223 336033.

## ■ AUTHOR INFORMATION

### Corresponding Author

\*J.P: tel, +420549496493; fax, +420549492443; e-mail, [jpinkas@chemi.muni.cz](mailto:jpinkas@chemi.muni.cz).

### ORCID

Jiri Pinkas: 0000-0002-6234-850X

### Notes

The authors declare no competing financial interest.

## ■ ACKNOWLEDGMENTS

The results of this research have been acquired within the CEITEC 2020 (LQ1601) project with financial contribution made by the MEYS CR within special support paid from the National Program for Sustainability II funds. CIISB research infrastructure project LM2015043 funded by MEYS CR is gratefully acknowledged for the financial support of the measurements at the CF X-ray Diffraction and Bio-SAXS and the Josef Dadok National NMR Centre. The authors thank Dr. M. Bittova for MS measurements, Dr. K. Novotny and L. Simonikova for ICP-OES analyses, and Dr. Z. Moravec for TG-DSC measurements.

## ■ REFERENCES

- (1) Livage, J.; Barboux, P.; Vandenborre, M. T.; Schmutz, C.; Taulelle, F. Sol-Gel Synthesis of Phosphates. *J. Non-Cryst. Solids* **1992**, *147–148*, 18–23.
- (2) Liebau, F.; Bissert, G.; Köppen, N. Synthese Und Kristallographische Eigenschaften Einiger Phasen Im System  $SiO_2-P_2O_5$ . *Z. Anorg. Allg. Chem.* **1968**, *359* (3–4), 113–134.
- (3) Makart, H. Untersuchungen an Siliciumphosphaten. *Helv. Chim. Acta* **1967**, *50* (2), 399–405.
- (4) Mayer, H. Die Kristallstruktur von  $Si_3O[PO_4]_6$ . *Monatsh. Chem.* **1974**, *105*, 46–54.
- (5) Poojary, D. M.; Borade, R. B.; Clearfield, A. Structural Characterization of Silicon Orthophosphate. *Inorg. Chim. Acta* **1993**, *208* (1), 23–29.
- (6) Poojary, D. M.; Borade, R. B.; Campbell, F. L., III; Clearfield, A. Crystal Structure of Silicon Pyrophosphate (Form I) from Powder Diffraction Data. *J. Solid State Chem.* **1994**, *112* (1), 106–112.
- (7) Styskalik, A.; Skoda, D.; Moravec, Z.; Babiak, M.; Barnes, C. E.; Pinkas, J. Control of Micro/mesoporosity in Non-Hydrolytic Hybrid Silicophosphate Xerogels. *J. Mater. Chem. A* **2015**, *3* (14), 7477–7487.
- (8) Sekine, M.; Okimoto, K.; Yamada, K.; Hata, T. Silyl Phosphites. 15. Reactions of Silyl Phosphites with  $\alpha$ -Halo Carbonyl Compounds. Elucidation of the Mechanism of the Perkow Reaction and Related Reactions with Confirmed Experiments. *J. Org. Chem.* **1981**, *46* (10), 2097–2107.
- (9) Jähnigen, S.; Brendler, E.; Böhme, U.; Kroke, E. Synthesis of Silicophosphates Containing  $SiO_6$ -Octahedra under Ambient Conditions – Reactions of Anhydrous  $H_3PO_4$  with Alkoxy-silanes. *Chem. Commun.* **2012**, *48* (62), 7675–7677.
- (10) Murugavel, R.; Prabusankar, G.; Walawalkar, M. G. Organic Soluble Silicophosphonate  $[RSi(OH)\{OP(O)(H)(OH)\}_2O]$  ( $R = (2,6-I-Pr_2C_6H_3)_3NSiMe_3$ ): The First Silicophosphonate Containing Free Si–OH and P–OH Groups. *Inorg. Chem.* **2001**, *40* (6), 1084–1085.
- (11) Vaugeois, Y.; De Jaeger, R.; Levalois-Mitjaville, J.; Mazzah, A.; Wörle, M.; Grütmacher, H. Synthesis and Structure of New Eight-Membered  $Si-O-\lambda^5\sigma^4-P$  Heterocycles. *New J. Chem.* **1998**, *22* (8), 783–785.
- (12) Goubeau, J.; Christe, K. O.; Teske, W.; Wilborn, W. Über Die Silicophosphorsäure Und Ihre Derivate. *Z. Anorg. Allg. Chem.* **1963**, *325* (1–2), 26–42.
- (13) Corriu, R. J. P.; Leclercq, D.; Mutin, P. H.; Sarlin, L.; Vioux, A. Nonhydrolytic Sol-Gel Routes to Layered metal(IV) and Silicon Phosphonates. *J. Mater. Chem.* **1998**, *8* (8), 1827–1833.
- (14) Styskalik, A.; Skoda, D.; Moravec, Z.; Abbott, J. G.; Barnes, C. E.; Pinkas, J. Synthesis of Homogeneous Silicophosphate Xerogels by Non-Hydrolytic Condensation Reactions. *Microporous Mesoporous Mater.* **2014**, *197*, 204–212.
- (15) Beckett, M. A.; Brassington, D. S.; Coles, S. J.; Hursthouse, M. B. Lewis Acidity of Tris(pentafluorophenyl)borane: Crystal and Molecular Structure of  $B(C_6F_5)_3 \cdot OPt_3$ . *Inorg. Chem. Commun.* **2000**, *3* (10), 530–533.
- (16) Beckett, M. A.; Brassington, D. S.; Light, M. E.; Hursthouse, M. B. Organophosphoryl Adducts of Tris(pentafluorophenyl)borane; Crystal and Molecular Structure of  $B(C_6F_5)_3 \cdot Ph_3PO$ . *J. Chem. Soc., Dalton Trans.* **2001**, 1768–1772.
- (17) Spek, A. L. Single-Crystal Structure Validation with the Program PLATON. *J. Appl. Crystallogr.* **2003**, *36* (1), 7–13.
- (18) Spek, A. L. *PLATON, A Multipurpose Crystallographic Tool*; University of Utrecht, Utrecht, The Netherlands, 1998.
- (19) Ishida, H.; Koenig, J. L. Vibrational Assignments of Organosilanetriols. II. Crystalline Phenylsilanetriol and Phenylsilanetriol- $d_3$ . *Appl. Spectrosc.* **1978**, *32* (5), 469–479.
- (20) Moss, G. P. Basic Terminology of Stereochemistry. *Pure Appl. Chem.* **1996**, *68* (12), 2193–2222.
- (21) Massey, A. G.; Park, J. Perfluorophenyl Derivatives of the Elements I. Tris(pentafluorophenyl)boron. *J. Organomet. Chem.* **1964**, *2*, 245–250.
- (22) Laposa, J. D.; Montgomery, C. Infrared Spectrum of Hexafluorobenzene Crystal at 77K. *Spectrochim. Acta* **1982**, *38* (11), 1109–1113.
- (23) Shurvell, H. F.; Faniran, J. A. Infrared Spectra of Triphenylboron and Triphenylborate. *Can. J. Chem.* **1968**, *46*, 2081–2087.
- (24) Erker, G. Tris(pentafluorophenyl)borane: A Special Boron Lewis Acid for Special Reactions. *J. Chem. Soc., Dalton Trans.* **2005**, *2* (11), 1883–1890.